Current-Programmed Control of Three Phase PWM AC-AC Buck Converter

Nam-Sup Choi*, and Yulong Li**

* Department of Electrical Engineering, Yosu National University, Yosu, Korea
(Tel : +82-61-659-3311; E-mail: nschoi@yosu.ac.kr)
**Department of Electrical Engineering, Yosu National University, Yosu, Korea
(Tel : +82-61-659-3311; E-mail: liyulong@yosu.ac.kr)

Abstract: In this paper, a new scheme of current programmed control for three phase PWM AC-AC converter is presented. Compared to duty-ratio voltage control, current programmed control has several advantages such as reduction of system order and inherent current protection. By considering only the magnitude components, the same scheme in the DC-DC converter can be extended to the three phase PWM AC-AC converter. Sensing the output voltage and the inductor current, an error signal will be generated by comparing the output voltage magnitude with a reference value. Then the error signal will be processed by a PI compensator to generate the current command. The converter switches will the change the state by a periodic clock pulse or at the instants when the inductor current magnitude reaches the current command. As an example case, the buck converter is treated. The converter analysis is carried out by applying the complex DQ circuit transformation to obtain basic physical insight into the converter operation and to establish some important characteristic equations for control purpose. The simulation with Simplorer shows the validity of the proposed scheme and the experimental results support the verification of the design.

Keywords: Current-Programmed Control, PWM AC-AC buck converter, DQ Transformation, DSP

1. INTRODUCTION

Current programmed control has been widely used in switching converters. Numerous attempts have been made to characterize this control scheme with small signal models. Current programmed DC-DC converter has been dealt with in many papers. In [1]-[2], complete analysis and discussion are presented for the three basic converters. In [3], a continuous-time current-mode control model together with sampling accuracy is discussed. In [4], a unified model is established for a current-programmed converter. In [5], a large-signal nonlinear control technique is proposed to control the duty ratio in one switching cycle.

However, the current programmed control for AC-AC switching converters has rarely been investigated. This paper proposes a practical current programmed control scheme for AC-AC switching converters.

By considering only the magnitude components, the similar scheme as in the DC-DC converter can be extended to AC-AC case. An error signal is generated by comparing the sensed output voltage magnitude with a reference value. Then the error signal may be processed by a PI compensator to generate the current command. The switches will be turned on by a clock pulse with a fixed frequency, and the turning off behavior occurs when the sensed inductor current magnitude reaches the current command.

The proposed current programmed control scheme has several advantages over conventional duty cycle control method. By processing the switching control signal with the current programmed controller, the small-signal control-to-output transfer function contains one less pole than that of duty cycle control, so the system order will be reduced. Such reduced system order may lead to easier controller design. Also, as the current programmed controller makes use of the sensed the inductor current information during normal converter operation, transistor failures due to excessive switch current can be prevented simply by setting the current reference value. Hence, inherent current protection is realized.

The proposed current programmed control will be well adopted into various converter topologies such as buck, boost, buck-boost, etc. The three phase PWM AC-AC buck converter is treated as an example in this paper [6]. Basic converter analysis is carried out by performing complex DQ transformation [7], thus some important characteristic relations are obtained for control purpose. The current programmed mode operation analysis together with the stability discussion is presented.

Finally, the Simplorer simulation and experiment results support the design and analysis.

2. SYSTEM DESCRIPTION

2.1 Operating principle

Fig. 1(a) shows the conventional duty cycle control diagram of the three phase PWM AC-AC buck converter. The output AC voltage is sensed and compared with a reference value to generate an error signal, which will be processed by a compensator. The switching control signal is made according to the compensator output.

Fig. 1(b) illustrates the proposed current programmed control diagram of the three phase PWM AC-AC buck converter. As seen in Fig. 1(b), the output AC voltage will be sensed to obtain the output voltage magnitude. This voltage magnitude is compared with a reference value to generate an error signal. The error signal then is processed by a PI controller to form the inductor current magnitude command. The control signal of the switches will be generated by the current programmed controller. The converter switches will be turned on by a clock with a fixed frequency, and the turning off instants will be determined by the inductor current magnitude. That is, the switches are turned off when the sensed inductor current magnitude reaches the current command.

By processing the switching control signal with the current programmed controller, the small-signal control-to-output transfer function $\hat{\mathbf{v}}_o(s)/\hat{\mathbf{i}}_c(s)$ contains one less pole than $\hat{\mathbf{v}}(s)/\hat{d}(s)$, so the system order will be reduced. Also, since the inductor current is directly controlled, the behavior is somewhat like the controlled current source, which will consequently make robust output.

2.2 Converter circuit

Fig. 2 shows the three-phase PWM Buck AC-AC converter. As seen in Fig. 2, the system requires six IGBTs.

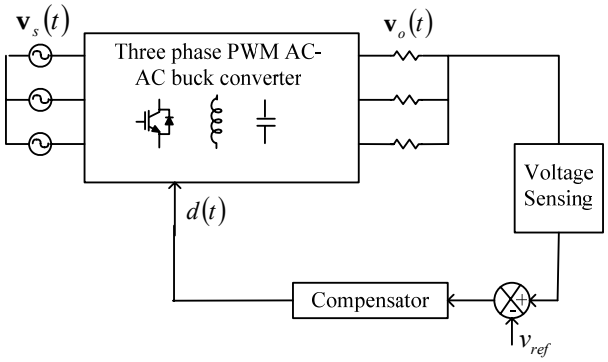

(a) Duty cycle voltage control

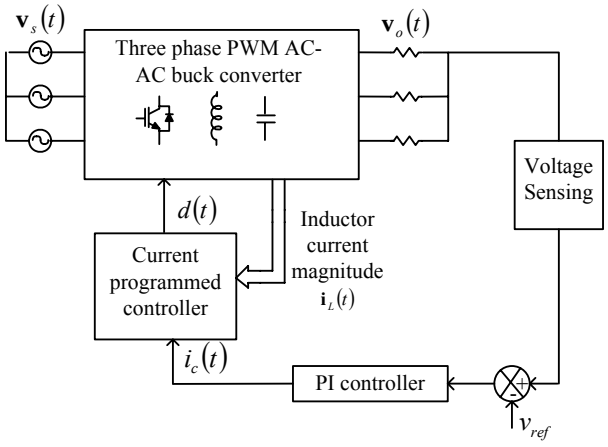

(b) Current programmed control

Fig. 1 Block diagram of the PWM AC-AC buck converter.

In Fig. 2, *r* represents parasitic resistance of *L*, and *R* is the load in which loss term of three-phase capacitors *C* is included. Also, *d* means the duty ratio of Q_1, Q_3 and Q_5 where they turn on or off in the way of simultaneous switching. Similarly, Q_2, Q_4 and Q_6 turn on or off simultaneously. Therefore, it should be noted that the system under analysis has only one control variable, *d*.

The source voltages with angular speed, ω are assumed ideal and balanced and are given as follows

$$\mathbf{v}_{sabc} = \begin{bmatrix} v_{sa} \\ v_{sb} \\ v_{sc} \end{bmatrix} = \sqrt{\frac{2}{3}} \cdot v_s \begin{bmatrix} \sin(\omega t) \\ \sin(\omega t - 2\pi/3) \\ \sin(\omega t + 2\pi/3) \end{bmatrix} \tag{1}$$

where v_s is the *rms* line-to-line AC source voltage.

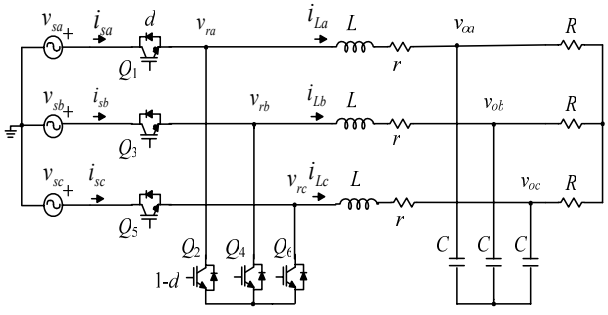

Fig 2. Three phase PWM AC-AC Buck converter topology.

3. CONVERTER ANALYSIS

3.1 Complex DQ transformation

The original circuit is partitioned into several basic subcircuits to be analyzed.

The vector $\mathbf{x}_{yabc}$ presents the three phase current and voltage of the circuit elements, is given by

$$\mathbf{x}_{yabc} = \begin{bmatrix} x_{ya} \\ x_{yb} \\ x_{yc} \end{bmatrix} . \tag{2}$$

For the inductor loop

$$\mathbf{v}_{rabc} - \mathbf{v}_{oabc} = r\mathbf{i}_{Labc} + L\frac{d}{dt}\mathbf{i}_{Labc} . \tag{3}$$

For the capacitor loop

$$\mathbf{i}_{Labc} = C\frac{d}{dt}\mathbf{v}_{oabc} + \frac{1}{R}\mathbf{v}_{oabc} . \tag{4}$$

Considering the circuit state according to the switching subintervals, in the subinterval when Q_1, Q_3, Q_5 are turned on, the circuit state will be shown in Fig. 3.

The corresponding equations are

$$\mathbf{v}_{rabc} = d\mathbf{v}_{sabc} . \tag{5}$$

By using synchronously rotating DQ transformation, the rotational three phase circuit shown in Fig. 2 can be transformed into the stationary circuit. A complex DQ transform is defined as follows

$$\mathbf{x}_{qdo} = \mathbf{K}\begin{bmatrix} x_a \\ x_b \\ x_c \end{bmatrix} = \begin{bmatrix} x_q \\ x_d \\ x_o \end{bmatrix} \tag{6}$$

$$\mathbf{K} = \sqrt{\frac{2}{3}}\begin{bmatrix} \cos(\omega t) & \cos\left(\omega t - \frac{2\pi}{3}\right) & \cos\left(\omega t + \frac{2\pi}{3}\right) \\ \sin(\omega t) & \sin\left(\omega t - \frac{2\pi}{3}\right) & \sin\left(\omega t + \frac{2\pi}{3}\right) \\ 1/\sqrt{2} & 1/\sqrt{2} & 1/\sqrt{2} \end{bmatrix} \tag{7}$$

$$\mathbf{x} = x_d + jx_q . \tag{8}$$

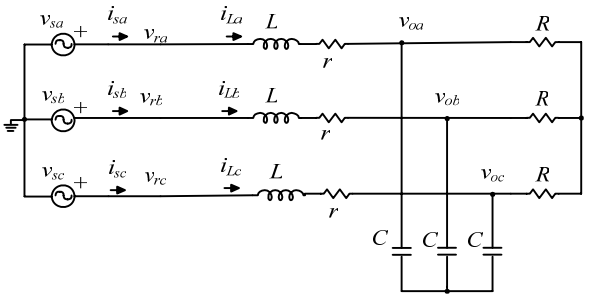

Fig. 3 Circuit state when Q_1, Q_3, Q_5 are turned on.

The source voltage can be transformed as

$$\mathbf{v}_s = v_{sd} + jv_{sq} = v_s \cdot \tag{9}$$

For equations (3), (4) and (5), the corresponding transformed equations will respectively be

$$\mathbf{v}_r - \mathbf{v}_o = r\mathbf{i}_L + L\frac{d}{dt}\mathbf{i}_L + j\omega L\mathbf{i}_L \tag{10}$$

$$\mathbf{i}_L = C\frac{d}{dt}\mathbf{v}_o + \frac{1}{R}\mathbf{v}_o + j\omega C\mathbf{v}_o \tag{11}$$

$$\mathbf{v}_r = d\mathbf{v}_s \cdot \tag{12}$$

In the above equations, the terms $j\omega L(j\omega C)$ do not mean conventional impedances but an element that represents the relationship of *d*- and *q*-components.

By using the complex DQ transformed equations of Eq. (10) through Eq. (12), the complex DQ transformed equivalent circuit can be drawn as shown in Fig. 4.

It should be noted that the equivalent circuit of Fig. 4 possesses the exact information on the presented system, which means, there is no loss in system information in the way of inducing the equivalent.

3.2 DC equivalent circuit

The steady state characteristics can be obtained by considering the DC equivalent circuit as shown in Fig. 5.

In steady state operation, the inductors seem to be short and capacitors open referring to Fig. 4 because all of the DC circuit variables imply DC values.

By pushing the source into the secondary side of the transformer and applying Ohm's Law and Kirchhoff's Law

$$\begin{cases} \mathbf{I}_L = \mathbf{V}_o\left(j\omega C + \dfrac{1}{R}\right) \\ D\mathbf{V}_s = \mathbf{I}_L(r + j\omega L) + \mathbf{V}_o \end{cases} \cdot \tag{13}$$

For convenience, some values are defined as follows

$$Q_L = \omega L/r\,, \quad Q_C = \omega CR\,, \quad \eta = r/R \cdot \tag{14}$$

The relationship between input and output voltage will be

$$\frac{\mathbf{V}_o}{\mathbf{V}_s} = \frac{D}{(1 - Q_L Q_C \eta + \eta) + j(Q_C\eta + Q_L\eta)} = \frac{D}{\rho\angle\alpha} \tag{15}$$

$$\rho = \sqrt{(1 - Q_L Q_C \eta + \eta)^2 + (Q_C\eta + Q_L\eta)^2} \cdot \tag{16}$$

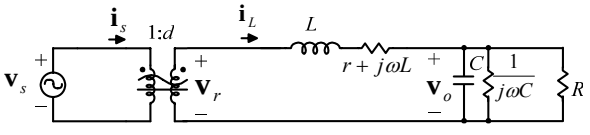

Fig. 4 Complex DQ transformed equivalent circuit.

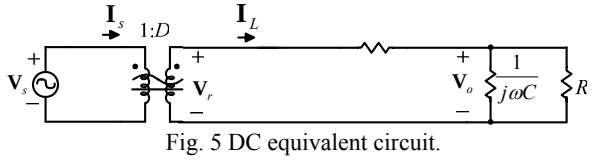

Fig. 5 DC equivalent circuit.

The magnitude relationship and voltage gain will be

$$\left|\frac{\mathbf{V}_o}{\mathbf{V}_s}\right| = \frac{D}{\rho} \cdot \tag{17}$$

It can be found from Eq. (15) and Eq. (17) that

1) Voltage gain of the presented three phase PWM AC-AC buck converter is similar to DC-DC converters, but modified by a factor of ρ.

2) Generally, Q_L, Q_C and η parts are comparably small, so the ρ factor almost has a unity value.

3.3 AC analysis

The AC analysis is carried out by introducing some perturbations to the control variable *d*. Therefore, the circuit variables consist of DC and AC components. The perturbed component is indicated by the diacritical mark '^' of the corresponding variable to distinguish it from the quiescent value as follows

$$\mathbf{i}_L = \mathbf{I}_L + \hat{\mathbf{i}}_L \;,\quad \mathbf{v}_o = \mathbf{V}_o + \hat{\mathbf{v}}_o \;,\quad d = D + \hat{d} \;. \tag{18}$$

The input voltage is not perturbed here. Fig. 6 shows the resultant small signal equivalent circuit obtained by applying the perturbation into the complex DQ transformed circuit of Fig. 4.

From Fig. 6, one can obtain

$$\frac{d}{dt}\begin{bmatrix}\hat{\mathbf{i}}_L \\ \hat{\mathbf{v}}_o\end{bmatrix} = \mathbf{A}\begin{bmatrix}\hat{\mathbf{i}}_L \\ \hat{\mathbf{v}}_o\end{bmatrix} + \begin{bmatrix}\mathbf{V}_s \\ 0\end{bmatrix}\hat{d} \tag{19}$$

where $\mathbf{A} = \begin{bmatrix} -(r + j\omega L) & -1 \\ 1 & -\left(j\omega C + \dfrac{1}{R}\right) \end{bmatrix}$. (20)

4. Current programmed control

4.1 Stability issue

Fig. 7 illustrates the inductor current magnitude waveform of the presented converter operating in the continuous conduction mode, where I_c is the current command.

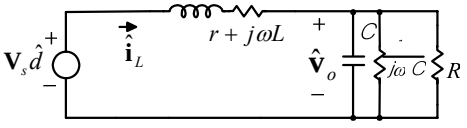

Fig. 6 AC equivalent circuit.

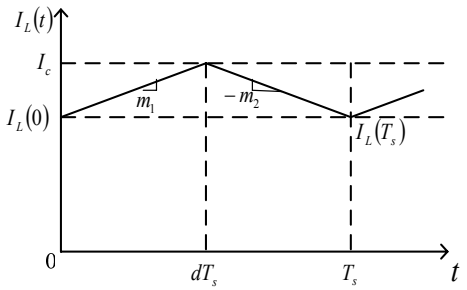

Fig. 7 Inductor current magnitude waveform of the presented converter in continuous conduction mode.

The changing slope in the two subintervals will be

$$m_1 = \frac{V_s - V_o}{L} \quad , \quad -m_2 = -\frac{V_o}{L} \cdot \tag{21}$$

Solving for the two subintervals

$$I_L(dT_s) = I_c = I_L(0) + m_1 dT_s \tag{22}$$

$$I_L(T_s) = I_L(dT_s) - m_2 d'T_s = I_L(0) + m_1 dT_s - m_2 d'T \cdot \tag{23}$$

where $d' = 1 - d$.

In steady state

$$I_L(0) = I_L(T_s), \quad d = D, \quad m_1 = M_1 \quad , \quad m_2 = M_2 \quad \cdot \tag{24}$$

Then

$$\frac{M_2}{M_1} = \frac{D}{D'} \tag{25}$$

where $D' = 1 - D$.

Introducing a small perturbation in $i_L(0)$, then

$$I_L(0) = I_{L0} + \hat{I}_L(0) \qquad |I_{L0}| >> |\hat{I}_L(0)| \cdot \tag{26}$$

Fig. 8 shows the details of the steady state and perturbed inductor magnitude waveforms near the peak value.

Based on Fig. 8, one can obtain

$$\hat{I}_L(0) = -m_1 \hat{d} T_s \tag{27}$$

$$\hat{I}_L(T_s) = -m_2 \hat{d} T_s \tag{28}$$

$$\hat{I}_L(T_s) = \hat{I}_L(0)\left(-\frac{m_2}{m_1}\right) = \hat{I}_L(0)\left(-\frac{D}{D'}\right) \cdot \tag{29}$$

A similar analysis can be performed for the next *n* switching periods, the perturbation becomes

$$\hat{I}_L(nT_s) = \hat{I}_L(0)\left(-\frac{m_2}{m_1}\right)^n = \hat{I}_L(0)\left(-\frac{D}{D'}\right)^n \cdot \tag{30}$$

Therefore, for stable operation of the current programmed controller, it is needed that $D/D' < 1$, which means $D<0.5$.

To avoid the stability problem, the control scheme is usually modified by adding a stabilizing ramp to the current command. A similar analysis can be performed. Fig. 9 shows the steady state and perturbed inductor current waveforms with the addition of stabilizing ramp.

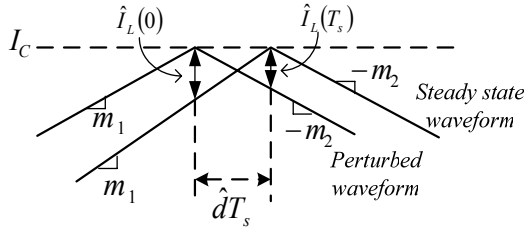

Fig. 8 Expanded view of steady state and perturbed inductor current magnitude waveform near peak value.

After *n* switching periods, the perturbation will be

$$\hat{I}_L(nT_s) = \hat{I}_L(0)\left(-\frac{m_2 - m_a}{m_1 + m_a}\right)^n = \hat{I}_L(0)\alpha^n \tag{31}$$

where m_a is the slope of the ramp and $\alpha = -\frac{m_2 - m_a}{m_1 + m_a}$.

It can be found that the stability will be dependent on the factor α. If the absolute value of α is less than unity, the converter will be stable.

For the buck converter, the maximal output voltage will be equal the input voltage, which means m_2 will have a maximal value $m_{2,max}$. For stability consideration, simply choose $m_a = 0.5 * m_{2,max}$. When the steady state duty ratio is near 0.5, it will satisfy the deadbeat control situation; while the duty ratio is near 1, it will suit $m_a = 0.5 * m_2$, which is the minimal value for m_a. This choice will lead to stability in full duty control.

4.3 Transfer function

Applying Laplace transform to Eq. (19) and Eq. (20), then

$$sC\hat{\mathbf{v}}_o(s) = -\left(j\omega C + \frac{1}{R}\right)\hat{\mathbf{v}}_o(s) + \hat{\mathbf{i}}_c(s) \cdot \tag{32}$$

An assumption is made that the inductor current magnitude perturbation is identical to the programmed current command perturbation. This is valid to the extent that the controller is stable, and that the magnitudes of the inductor current ripple and stabilizing ramp waveform are sufficiently small.

$$\hat{\mathbf{i}}_L(s) \approx \hat{\mathbf{i}}_c(s) \cdot \tag{33}$$

Substituting Eq. (32) into Eq. (31) and rearranging terms

$$\frac{\hat{\mathbf{v}}_o(s)}{\hat{\mathbf{i}}_c(s)} = \frac{1}{j\omega C + \frac{1}{R} + sC} \cdot \tag{34}$$

From Eq. (34), it can be found that the small-signal control-to-output transfer function $\hat{\mathbf{v}}_o(s)/\hat{\mathbf{i}}_c(s)$ contains only one pole, so the system order is reduced.

The magnitude relationship will be

$$\left|\frac{\hat{\mathbf{v}}_o(s)}{\hat{\mathbf{i}}_c(s)}\right| = \frac{1}{\sqrt{\omega^2 C^2 + \left(\frac{1}{R} + sC\right)^2}} \cdot \tag{35}$$

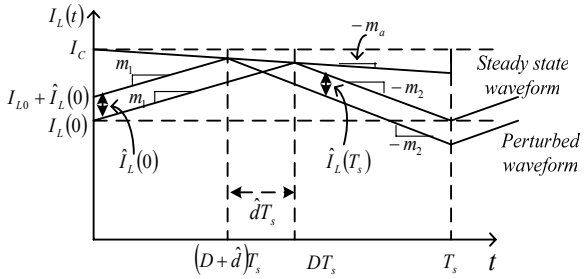

Fig. 9 Steady state and perturbed inductor current magnitude waveforms in the presence of a stabilizing ramp.

In decibel,

$$20\log_{10}\left|\frac{\hat{\mathbf{v}}_o}{\hat{\mathbf{i}}_c}\right| = 10\log_{10} F(s) \tag{36}$$

$$F(s) = \frac{\frac{1}{R^2}+C^2\omega^2}{(Cs+1/R)^2+C^2\omega^2} = \frac{\frac{1}{R^2}+C^2\omega^2}{1+\frac{s}{Q\omega_0}+\left(\frac{s}{\omega_0}\right)^2} \tag{37}$$

where $\omega_0 = \frac{\sqrt{1+R^2C^2\omega^2}}{RC}$, $Q = \sqrt{1+R^2C^2\omega^2}/2$. (38)

It can be seen from Eq. (37) and Eq. (38) that *F(s)* predicts quadratic pole response. While in low frequency operation, it mainly shows proportional effect.

5. SIMULATION AND EXPERIMENT

To confirm the validity of the design and analysis for the current programmed three phase PWM AC-AC buck converter, some simulations are carried out by using Simplorer. The circuit parameters are as follows

v_s =100 V, f=60 Hz, L =1.5 mH,
r=0.01 Ω, C=20 μF, R=5 Ω.

Also, the switching frequency is 5kHz.

During the simulation process, the magnitude components are determined by the next two equations.

$$i_{L,mag} = \sqrt{\frac{2}{3}\left(i_{La}{}^2 + i_{Lb}{}^2 + i_{Lc}{}^2\right)} \tag{39}$$

$$v_{o,mag} = \sqrt{\frac{2}{3}\left(v_{oa}{}^2 + v_{ob}{}^2 + v_{oc}{}^2\right)} \tag{40}$$

where $i_{L,mag}$ and $v_{o,mag}$ present the instantaneous inductor current magnitude and output voltage magnitude; i_{La}, i_{Lb}, i_{Lc} mean the three phase inductor current, and v_{oa}, v_{ob}, v_{oc} mean the three phase output voltage respectively.

Fig. 10 shows the simulation waveforms when the reference voltage(v_{ref}) is set to be 40V. As shown in the figure, it can be seen that the output voltage magnitude well follows the reference voltage.

An experiment setup is also made to support the analysis and simulation result of the PWM AC-AC buck converter with current programmed control. The actual values of the circuit elements are the same with the simulation.

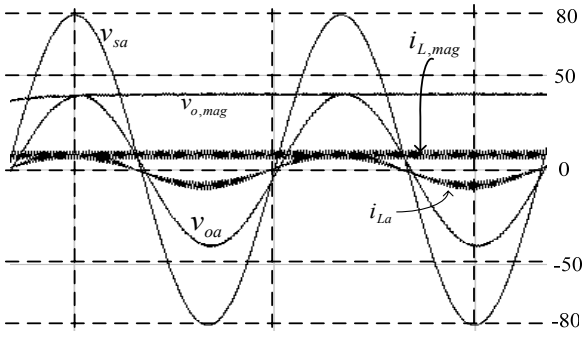

Fig. 10 Voltage and current waveforms when v_{ref} = 40V.

TMS320F2812 digital signal processor (DSP) is applied in the experiment [8]. The TMS320F2812 DSP includes 16 internal A/D converters, of which 6 are used to read the sensed three phase inductor currents and output voltages.

Fig. 11 shows the steady state input and output voltage waveforms. In Fig. 11, the output voltage is set to be a magnitude reference of 53V. From Fig. 11, it can be seen that the designed current programmed converter operates well.

Fig. 12 shows the dynamics waveforms of the inductor current, input voltage and output voltage when the voltage reference set to change from 32V to 53V. It can be seen from Fig. 12 that the output well follows the reference voltage, and the transient time is about one cycle.

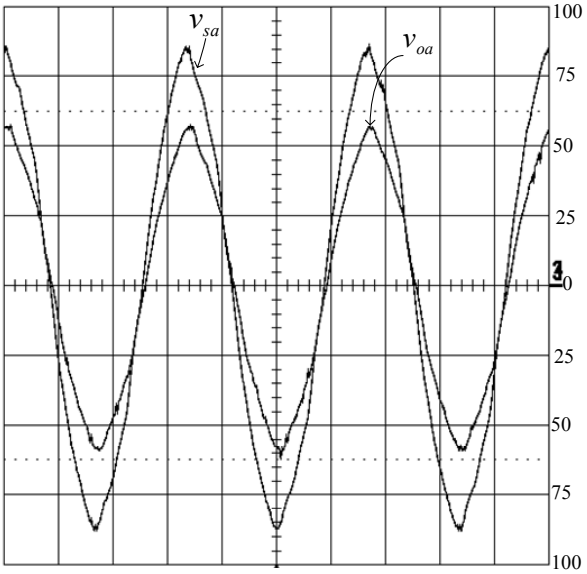

Fig. 11 Steady state input and output voltage waveforms (25V/div, 5ms/div).

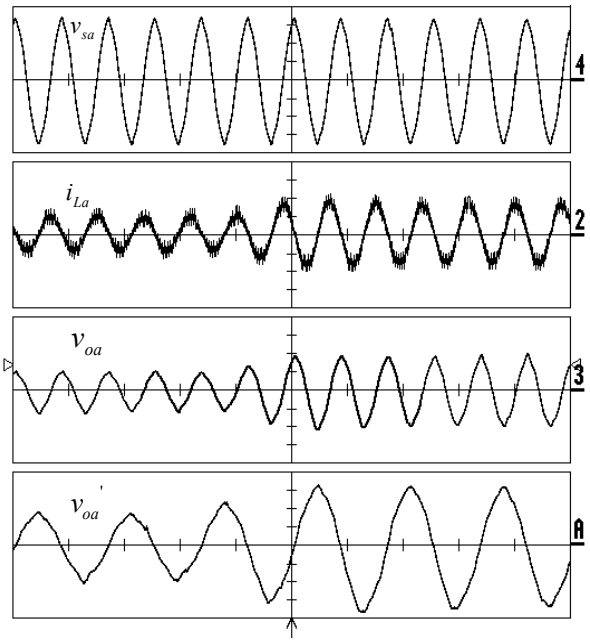

Fig. 12 Dynamics waveforms of voltage reference change v_{sa}(25V/div, 20ms/div); i_{La}(5A/div, 20ms/div); v_{oa}(25V/div, 20ms/div); v_{oa}'(17V/div, 10ms/div).

Fig. 13 shows the dynamics waveforms of the input voltage, output voltage and inductor current when the load resistance is set to change from 5Ω to 2.5Ω. As seen in Fig. 13, the transient time is about 3 cycles.

7. CONCLUSION

This paper deals with the current programmed control of three phase PWM AC-AC buck converter. The same scheme of DC-DC converter in current programmed mode is extended to AC-AC case by considering the magnitude components. A detailed analysis is carried out by using complex DQ transform method. Operation of the presented converter in current programmed mode and stability discussion are investigated.

Practical realization of the current programmed controller is achieved by using DSP programming. The experimental waveforms well support the design and analysis.

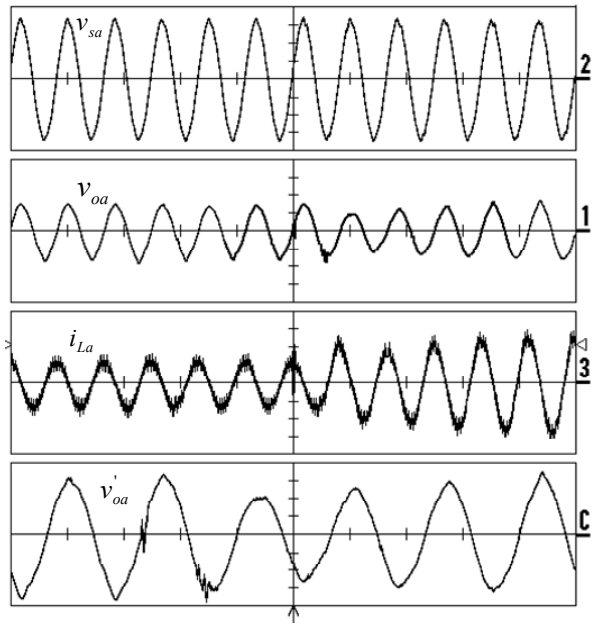

Fig. 13 Dynamics waveforms of load resistance change
v_{sa}(25V/div, 20ms/div); i_{La}(5A/div, 20ms/div);
v_{oa}(25V/div, 20ms/div); v_{oa}'(17V/div, 10ms/div).

REFERENCES

[1] R. D. Middlebrook, "Modeling Current Programmed Buck and Boost Regulators," *IEEE Transactions on Power Electronics*, Vol. 4, January 1989, pp. 36-52.

[2] R. D. Middlebrook, "Topics in Multiple-Loop Regualators and Current-Mode Programming," *IEEE Power Electronics Specialists Conference*, 1985 Record, pp. 716-732.

[3] R. Ridley, "A New Continuous-Time Model for Current-Mode Control," *IEEE Transactions on Power Electronics*, Vol. 6, No. 2, April 1991, pp. 271-280.

[4] F. D. Tan and R. D. Middlebrook, "Unified Modeling and Measurement of Current-Programmed Converters," *IEEE Power Electronics Specialists Conference*, 1993 Record, pp. 503-511.

[5] K. Smedley and S. Cuk, "One-Cycle Control of Switching Converters," *IEEE Power Electronics Specialists Conference*, 1991 Record, pp. 888-896.

[6] Kwon, B.-H.; Min, B.-D. and Kim, J.-H., 'Novel topologies of AC choppers'. *Electric Power Applications, IEE Proceedings* Volume 143, Issue 4, July 1996, pp. 323-330.

[7] Soo-Bin Han; Gyu-Hyeong Choi; Bong-Man Jung and Soo-Hyun Choi, 'Vector-transformed circuit theory and application to converter modeling/analysis'. *Power Electronics Specialists Conference*, 1998 Record, Vol. 1, pp. 538-544.

[8] David M. Alter, "Thermoelectric Cooler Control Using a TMS320F2812 DSP and a DVR592 Power Amplifier," *Texas Instruments DSP Applications*, Semiconductor Group, February 2003.